ELSEVIER

Journal of Hazardous Materials B79 (2000) 189–208

Journal of Hazardous Materials

www.elsevier.nl/locate/jhazmat

Thermodynamic driving forces for PAH isomerization and growth during thermal treatment of polluted soils

Christopher J. Pope [1], William A. Peters [*], Jack B. Howard

Department of Chemical Engineering, Center for Environmental Health Sciences, and Energy Laboratory, Massachusetts Institute of Technology, Cambridge, MA 02139-4307, USA

Received 23 September 1999; received in revised form 18 May 2000; accepted 19 May 2000

Abstract

For a limiting case of thermodynamic equilibrium, the importance of two classes of thermal chemical reactions that modify the structure and bioactivity of polycyclic aromatic hydrocarbons (PAH) was assessed computationally. These reactions are molecular weight (MW) growth by acetylene addition, and intramolecular rearrangement (isomerization). Temperatures (300–1100°C), and the chemical environment (C_2H_2/H_2 molar ratios) were selected for relevancy to thermal treatment of PAH-contaminated soils under oxygen-free conditions. Molecular mechanics methods [MM3(92)] were used to compute thermochemical properties for calculation of equilibrium constants, i.e., heats of formation, standard entropies, and heat capacities for 30 PAH with empirical formulae $C_{14}H_{10}$, $C_{16}H_{10}$, $C_{18}H_{10}$, $C_{18}H_{12}$, $C_{20}H_{10}$, and $C_{20}H_{12}$. Included were 11 PAH containing only six-membered rings and 19 PAH containing both five- and six-membered rings. For each of these PAH the calculations predict that with increasing temperature, isomerization increases the "complexity" of the PAH mixture, i.e., the relative abundance of each PAH isomer in the mixture other than the most stable isomer, increases. Isomerization also partially transforms non-mutagens to mutagens, e.g., pyrene and benzo[*e*]pyrene to fluoranthene and benzo[*a*]pyrene, respectively, and partially converts cyclopenta[*c,d*]pyrene (CPEP) and chrysene, both human cell mutagens, to one and three additional human cell mutagens, respectively. Acetylene addition transforms the non-mutagens phenanthrene and pyrene to the mutagens triphenylene and CPEP, respectively. Some of the predicted PAH have been observed elsewhere among the products of aromatics pyrolysis. This study elucidates PAH reactivity for comparison

[*] Corresponding author. Room E40-451, Energy Laboratory, Massachusetts Institute of Technology, 77 Massachusetts Avenue, Cambridge, MA 02139-4307, USA. Tel.: +1-617-253-3433; fax: +1-617-253-8013.
E-mail address: peters@mit.edu (W.A. Peters).

[1] Present Address: Sandia National Laboratories P.O. Box 969, Livermore, CA, USA.

PII: S0304-3894(00)00267-3

with measurements, and identifies PAH reactions to be monitored and avoided in soil thermal decontamination and other waste remediation processes.

Keywords: Soil; Thermal decontamination; PAH; Thermodynamics; Molecular mechanics

1. Introduction

Controlled thermal treatment is an effective means for destruction and/or removal of organic pollutants from soil. However, soil heating may generate unwanted by-products, e.g., from soil pyrolysis or incomplete destruction of the contaminant. Adverse chemical reactions are possible at temperatures from as low as 300°C to 500°C, owing to catalysis by soil minerals, to as high as 1000°C or more, where vapor phase pyrolysis and partial oxidation proceed readily. Parasitic chemistries may be especially problematical in thermal remediation of soils contaminated by polycyclic aromatic hydrocarbons (PAH). Some PAH are mutagens [1,2] or carcinogens, or both, but bioactivity depends upon PAH molecular structure. During soil thermal treatment, PAH chemical reactions may decontaminate PAH, or transform them to toxic PAH or other hazardous substances that

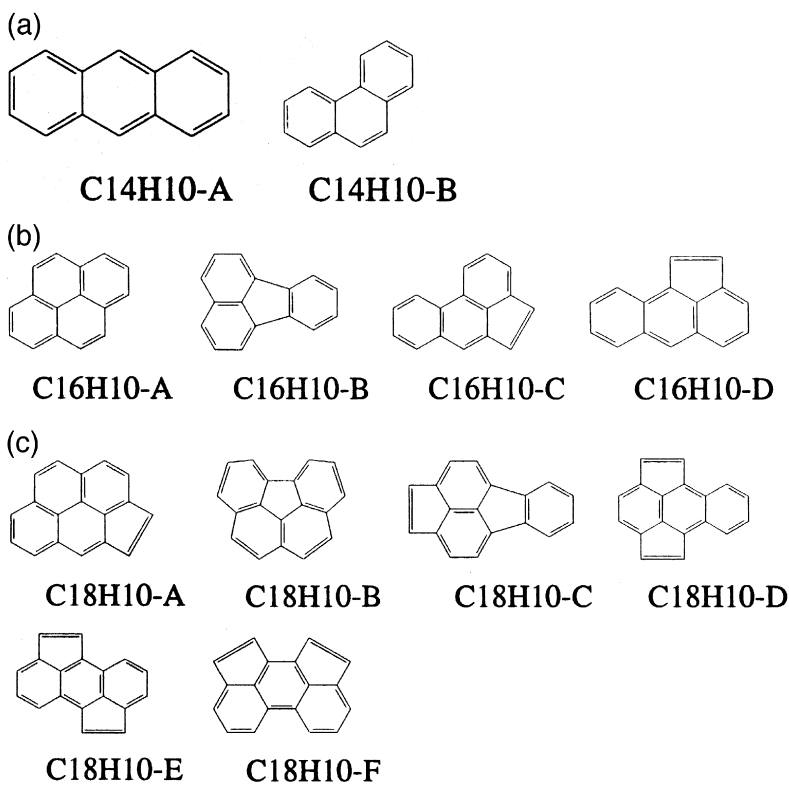

Fig. 1. Structural formulae for PAH compounds considered in the present work: (a) $C_{14}H_{10}$, (b) $C_{16}H_{10}$, (c) $C_{18}H_{10}$, (d) $C_{18}H_{12}$, (e) $C_{20}H_{10}$, and (f) $C_{20}H_{12}$. Compound names are given in Table 1.

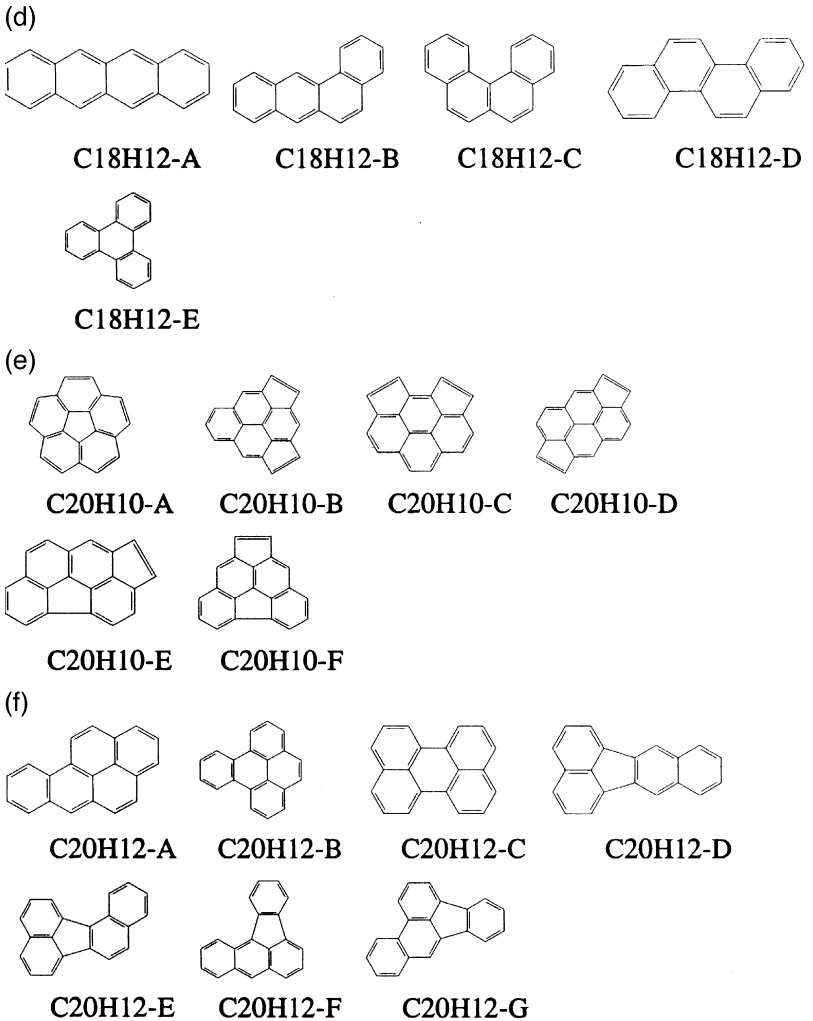

Fig. 1 (*continued*).

demand further cleanup to avoid unacceptable process effluents. An understanding of the propensity of PAH to undergo such reactions during soil thermal treatment is important in achieving efficient thermal cleaning of PAH-polluted soils without emitting hazardous by-products.

Soil thermal treatment has physical and chemical features similar to those encountered in other thermal processing environments such as combustion and pyrolysis, where PAH can grow in molecular weight (MW) by addition of acetylene (C_2H_2) [3–5], as well as intramolecular rearrangements [1,6–9], which interconvert PAH isomers. To better assess the possibility that PAH reactions during soil thermal treatment may give rise to toxic or other unwanted by-products, we performed a systematic study of the

thermochemistry of plausible PAH transformation reactions for chemical environments and temperatures of practical interest. To that end, thermodynamic properties ($\Delta H_f°$, $S°$, $C_p°$) for 30 unsubstituted PAH with masses ranging from 178 to 252 amu were computed in the present study using MM3(92) [10], which has been shown to reliably predict heats of formation of PAH [10], the heat of formation [11,12] and heat capacity [13] of the large aromatic molecule C_{60} fullerene, and the advantage [14], i.e., the lower standard enthalpy of formation, of the known structure of $C_{36}H_{12}$ decacyclene [15] over other candidate structures. Relative stabilities of groups of PAH isomers with the same empirical formula ($C_{14}H_{10}$, $C_{16}H_{10}$, $C_{18}H_{10}$, $C_{18}H_{12}$, $C_{20}H_{10}$, and $C_{20}H_{12}$) were determined as a function of temperature. For thermodynamic studies at high temperatures, the effects of entropy must be included. Knowledge of the heats of formation of the PAH is insufficient, and can even lead to erroneous results [16]. The calculation of vibrational frequencies, needed for obtaining standard entropies and heat capacities, can be very expensive for large molecules when higher levels of theory are used. The MM3(92) method provides all the information needed for the present study with more than sufficient accuracy at reasonable computational cost.

Acetylene and molecular hydrogen released by decomposition of the soil or its contaminants may promote PAH MW growth. Thus, the partial pressures of C_2H_2 and H_2 under conditions relevant to soil thermal treatment are needed to assess driving forces for PAH MW growth. From studies on specimens of the same soil with [17,18] and without [19] pyrene contamination, the amounts of CH_4, C_2H_2, and C_2H_4 were little changed (up to $\sim 20\%$) by the addition of pyrene to the soil. Therefore, the results of an experimental study of thermal treatment of a neat synthetic soil matrix [19] prepared elsewhere [20] to reflect attributes of soils at US Superfund Sites, were used to determine, as accurately as possible, concentrations of C_2H_2 and H_2, for use in computations to determine equilibrium concentrations of reactants and products for representative PAH MW growth reactions. This soil matrix has been used in various experiments [17–19,21,22].

2. PAH species and their thermochemical properties

The aromatic species considered here are all unsubstituted PAH containing either 6-membered rings only (PAH6) or five- and six-membered rings (PAH5/6). All the possible PAH6 are included, as are PAH5/6 most likely to be stable, which are those with ace-rings or with a five-membered ring in which each carbon atom is part of an adjoining six-membered ring, such as in fluoranthene, benzo[*ghi*]fluoranthene, or corannulene (dibenzo[*ghi*,*mno*]fluoranthene). The molecular structures of the PAH are given in Fig. 1. For $C_{20}H_{12}$, the only PAH5/6 structures considered are those with a fluoranthene-type five-membered ring. The mutagenicities of the PAH in human cell [2] and bacterial cell [1] assays are listed in Table 1, along with the IUPAC names of the PAH.

Values for $H_f°$, $S°$, and $C_p°$ for these PAH, calculated with the molecular mechanics program MM3(92) are presented in Table 2. The heats of formation and entropies are for

Table 1
Mutagenicity and IUPAC nomenclature for the PAH species shown in Fig. 1. Notation for mutagenicity in human cell test[2]: + = positive, − = negative, x = not tested. Results for bacterial assay[1]: y = positive, n = negative

Species name	Mutagenicity	IUPAC name(s)
C14H10-A	x	anthracene
C14H10-B	–	phenanthrene
C16H10-A	−,n	pyrene
C16H10-B	−,y	fluoranthene
C16H10-C	x,y	acephenanthrylene, cyclopenta[*jk*]phenanthrene
C16H10-D	x	aceanthrylene, cyclopenta[*de*]anthracene
C18H10-A	+,y	cyclopenta[*cd*]pyrene
C18H10-B	−,y	benzo[*ghi*]fluoranthene
C18H10-C	x	cyclopenta[*cd*]fluoranthene
C18H10-D	x	cyclopenta[*fg*]aceanthrylene, dicyclopenta[*de,mn*]anthracene
C18H10-E	x	cyclopenta[*hi*]aceanthrylene, dicyclopenta[*de,kl*]anthracene
C18H10-F	x	cyclopenta[*hi*]acephenanthrylene, dicyclopenta[*jk,mn*]phenanthrene
C18H12-A	x	naphthacene
C18H12-B	+	benz[*a*]anthracene
C18H12-C	+	benzo[*c*]phenanthrene
C18H12-D	+	chrysene
C18H12-E	+	triphenylene
C20H10-A	x	corannulene, dibenzo[*ghi,mno*]fluoranthene
C20H10-B	x	dicyclopenta[*cd,mn*]pyrene
C20H10-C	x	dicyclopenta[*cd, fg*]pyrene
C20H10-D	x	dicyclopenta[*cd, jk*]pyrene
C20H10-E	x	indeno[6,5,4,3-*ghij*]fluoranthene
C20H10-F	x	indeno[1,7,6,5-*fghi*]fluoranthene
C20H12-A	+,y	benzo[*a*]pyrene
C20H12-B	x	benzo[*e*]pyrene
C20H12-C	−	perylene
C20H12-D	+,y	benzo[*k*]fluoranthene
C20H12-E	+	benzo[*j*]fluoranthene
C20H12-F	x	benzo[*a*]fluoranthene
C20H12-G	+	benzo[*b*]fluoranthene

an ideal gas at standard temperature and pressure, i.e., 298 K and 1 atm. As in previous work [12], MM3(92) predicts a planar structure for $C_{18}H_{10}$-B; the value of S° in Table 2 is corrected to account for the change in symmetry due to the actual structure being non-planar. Calculations for each of the PAH required ~5–15 CPU min on a DEC 5000 workstation, with three to six successive runs performed to ensure convergence. The experimental heats of formation for $C_{14}H_{10}$-A, $C_{14}H_{10}$-B, $C_{16}H_{10}$-A, $C_{16}H_{10}$-B, and the five $C_{18}H_{12}$ species [23] are used in the following thermodynamic analyses.

3. Isomerization as a pathway for PAH modification

For temperatures pertinent to soil thermal decontamination (227°C to 1227°C) [19], Table 3 presents the relative stabilities of each selected PAH as the equilibrium ratio of

Table 2
Thermochemical properties for PAH in Fig. 1, calculated by MM3(92). Units: $H_f°$ in kcal/mol; $S°$ and $C_p°$ in cal/mol K

Species	$H_f°$	$S°$ (298)	$C_p°$, 300 K	$C_p°$, 400 K	$C_p°$, 500 K	$C_p°$, 600 K	$C_p°$, 800 K	$C_p°$, 1000 K	$C_p°$, 1500 K
C14H10-A	54.97	94.88	45.22	59.62	71.76	81.64	96.25	106.28	120.67
C14H10-B	50.41	96.61	45.17	59.52	71.65	81.54	96.16	106.21	120.62
C16H10-A	57.83	97.59	49.37	65.22	78.55	89.38	105.34	116.20	131.60
C16H10-B	71.20	100.59	49.92	65.85	79.19	89.98	105.80	116.55	131.77
C16H10-C	76.81	102.15	50.21	66.15	79.48	90.23	105.97	116.66	131.81
C16H10-D	82.77	105.16	50.33	66.25	79.55	90.29	106.01	116.69	131.83
C18H10-A	87.26	104.97	54.48	71.90	86.40	98.09	115.14	126.64	142.77
C18H10-B	93.57	105.62	54.35	71.74	86.23	97.92	114.99	126.52	142.72
C18H10-C	110.12	105.85	55.07	72.55	87.05	98.68	115.59	126.96	142.93
C18H10-D	122.20	106.22	55.56	72.97	87.40	98.98	115.78	127.09	142.98
C18H10-E	109.47	105.34	55.34	72.78	87.25	98.86	115.72	127.06	142.97
C18H10-F	103.13	105.15	55.18	72.65	87.15	98.79	115.68	127.03	142.96
C18H12-A	75.74	108.69	57.62	75.79	91.06	103.48	121.80	134.32	152.17
C18H12-B	68.20	111.84	57.53	75.66	90.92	103.35	121.69	134.23	152.11
C18H12-C	71.50	110.66	57.34	75.50	90.81	103.28	121.66	134.23	152.12
C18H12-D	66.62	111.19	57.62	75.68	90.91	103.32	121.64	134.19	152.07
C18H12-E	67.17	110.80	57.69	75.70	90.91	103.31	121.61	134.14	152.03
C20H10-A	119.97	105.42	59.56	78.24	93.75	106.26	124.50	136.75	153.80
C20H10-B	122.33	109.00	59.62	78.60	94.26	106.80	124.94	137.06	153.93
C20H10-C	118.46	108.48	59.52	78.45	94.11	106.66	124.84	137.00	153.91
C20H10-D	119.21	108.57	59.62	78.61	94.28	106.83	124.96	137.08	153.94
C20H10-E	135.61	112.66	60.06	78.88	94.43	106.91	124.99	137.10	153.96
C20H10-F	136.04	110.96	60.16	78.97	94.51	106.98	125.05	137.15	153.99
C20H12-A	75.33	114.60	61.83	81.37	97.81	111.18	130.83	144.19	163.06
C20H12-B	73.12	114.32	61.82	81.33	97.75	111.12	130.78	144.13	163.01
C20H12-C	78.30	113.89	61.90	81.41	97.83	111.19	130.82	144.17	163.03
C20H12-D	86.04	114.29	62.23	81.94	98.44	111.79	131.33	144.57	163.26
C20H12-E	88.96	116.50	62.38	82.00	98.44	111.76	131.28	144.51	163.21
C20H12-F	91.75	116.35	62.44	82.05	98.49	111.81	131.31	144.54	163.23
C20H12-G	84.10	115.81	62.24	81.89	98.37	111.72	131.27	144.52	163.23

the concentration of that PAH compound to the concentration of the most stable PAH isomer of the same empirical formula. The computer program THERM [24] was used with the thermochemical data of Table 2 to calculate the equilibrium constants needed to estimate these concentration ratios. For each PAH of a given empirical formula in Table 1 there are two or more isomers, one of which remains the most stable over the entire range of temperatures studied here. For several temperatures from 500 to 1500 K, Table 4 presents the mole fraction of each isomeric mixture accounted for by the most stable isomer. The "mixture" is all PAH isomers from Fig. 1 of the stated empirical formula. Table 4 clearly shows that for a given compound, the most stable isomer accounts for less and less of the mixture with increasing temperature. For $C_{16}H_{10}$, $C_{18}H_{10}$, $C_{18}H_{12}$ and $C_{20}H_{10}$ (Table 4), there is also a general trend of the most stable isomer accounting for less of the mixture with increasing MW at a fixed temperature. These findings have significant practical implications. They show that during soil thermal treatment, the

number and concentration of PAH contaminants may change because one or more initial PAH pollutants are transformed to several isomers, especially at elevated temperatures and for higher MW PAH. The extent to which the isomerizations predicted by equilibrium calculations will be realized depends upon whether or not isomerization kinetics are rapid enough at the prevailing physical and chemical conditions. For example, PAH isomerizations exhibit high activation energies in the gas phase [1,9], suggesting that equilibration of isomers will become more favored at higher treatment temperatures. If soil mineral matter catalyzes PAH isomerization, equilibration may become possible at lower temperatures *if* the PAH remain in contact with the soil for sufficient time. This in turn depends upon the relative rates of mass transfer of PAH away from the soil vs. chemical isomerization on the soil. Higher temperatures would again favor a closer approach to the situation predicted by equilibrium because of the typically stronger temperature dependence of chemical vs. mass transfer rates. One plausible role for soil in promoting PAH isomerizations is in stabilizing the structurally complex intermediates expected in some reaction trajectories. For example, rearrangements involving PAH6 would probably proceed through an intermediate having a seven-membered ring [8].

4. The chemical environment for MW growth processes

PAH undergo MW growth by acetylene addition giving H_2 as a by-product. Thus, ambient partial pressures of C_2H_2 and H_2, as well as temperature are needed to compute thermodynamic driving forces for this growth pathway. Bucalá et al. [19] measured cumulative yields of CO, CO_2, CH_4, C_2H_2, C_2H_4, C_2H_6, and tars from rapid heating (c. 1000°C/s) of a Superfund related soil matrix, as affected by temperature (350°C to 1050°C), and best fitted the yield data to global kinetic rate expressions. Volatiles concentrations or partial pressures were not directly measured, but these quantities can be estimated for the present calculations. The approach was to use the kinetic parameters obtained by Bucalá et al. [19] to predict the continuous variation of cumulative volatiles yields with temperature–time history. Volatiles concentrations at the soil particle surface were then deduced by assuming the cumulative yields are proportional to ambient (soil surface) volatiles concentrations integrated over time. This analysis assumed that any effects of heat or mass transfer resistances on the observed volatiles yields are negligible or enfolded in the global kinetic rate expressions. In actuality, rates of diffusive mass transfer are species dependent, owing to the dependence of the diffusion coefficient on species MW and on a measure of the probability of species collisions contributing to mass transfer (i.e., the cross-section for diffusion).

Because Bucalá et al. [19] did not directly measure H_2 yields, their hydrogen elemental balances [19] were analyzed to obtain a reasonable estimate for the amount of H_2 produced by soil pyrolysis. The amount of oxygen not accounted for in the element balance was assumed to be from H_2O formed chemically during pyrolysis (in addition to the H_2O from the moisture). The amount of elemental hydrogen not accounted for by H in this water plus that assayed in other products was then assumed to be H_2. The resulting molar concentrations and relative amounts of H_2 and C_2H_2 calculated by these

Table 3
Equilibrium ratios of PAH to the most stable isomer of the same empirical formula (see text for discussion)

T (K)	T (°C)	[C14H10-A]/[C14H10-B]
500	227	1.500E − 03
700	427	7.562E − 03
800	527	1.255E − 02
900	627	1.863E − 02
1000	727	2.557E − 02
1100	827	3.314E − 02
1200	927	4.114E − 02
1300	1027	4.942E − 02
1500	1227	6.628E − 02

T (K)	T (°C)	[C16H10-B]/[C16H10-A]	[C16H10-C]/[C16H10-A]	[C16H10-D]/[C16H10-A]
500	227	6.705E − 06	5.280E − 08	5.995E − 10
700	427	3.297E − 04	1.334E − 05	8.469E − 07
800	527	1.122E − 03	7.597E − 05	8.265E − 06
900	627	2.920E − 03	2.953E − 04	4.885E − 05
1000	727	6.289E − 03	8.775E − 04	2.031E − 04
1100	827	1.180E − 02	2.144E − 03	6.532E − 04
1200	927	1.997E − 02	4.522E − 03	1.732E − 03
1300	1027	3.118E − 02	8.512E − 03	3.958E − 03
1500	1227	6.373E − 02	2.347E − 02	1.488E − 02

T (K)	T (°C)	[C18H10-B]/[C18H10-A]	[C18H10-C]/[C18H10-A]	[C18H10-D]/[C18H10-A]	[C18H10-E]/[C18H10-A]	[C18H10-F]/[C18H10-A]
500	227	2.400E − 03	1.642E − 10	1.064E − 15	2.478E − 10	1.320E − 07
700	427	1.454E − 02	1.239E − 07	2.674E − 11	1.579E − 07	1.346E − 05
800	527	2.546E − 02	9.895E − 07	6.414E − 10	1.200E − 06	5.760E − 05
900	627	3.933E − 02	4.997E − 06	7.627E − 09	5.832E − 06	1.792E − 04
1000	727	5.566E − 02	1.830E − 05	5.546E − 08	2.072E − 05	4.453E − 04
1100	827	7.390E − 02	5.299E − 05	2.818E − 07	5.859E − 05	9.398E − 04
1200	927	9.356E − 02	1.287E − 04	1.093E − 06	1.395E − 04	1.754E − 03
1300	1027	1.142E − 01	2.729E − 04	3.449E − 06	2.911E − 04	2.976E − 03
1500	1227	1.570E − 01	9.100E − 04	2.171E − 05	9.456E − 04	6.948E − 03

T (K)	T (°C)	[C18H12-A]/[C18H12-D]	[C18H12-B]/[C18H12-D]	[C18H12-C]/[C18H12-D]	[C18H12-E]/[C18H12-D]		
500	227	1.568E − 03	5.186E − 03	4.371E − 03	2.835E − 01		
700	427	6.997E − 03	2.555E − 02	1.883E − 02	3.851E − 01		
800	527	1.119E − 02	4.208E − 02	2.970E − 02	4.237E − 01		
900	627	1.614E − 02	6.204E − 02	4.235E − 02	4.562E − 01		
1000	727	2.166E − 02	8.466E − 02	5.626E − 02	4.839E − 01		
1100	827	2.756E − 02	1.092E − 01	7.099E − 02	5.077E − 01		
1200	927	3.371E − 02	1.350E − 01	8.619E − 02	5.283E − 01		
1300	1027	4.000E − 02	1.616E − 01	1.016E − 01	5.464E − 01		
1500	1227	5.262E − 02	2.156E − 01	1.322E − 01	5.763E − 01		

T (K)	T (°C)	[C20H10-A]/[C20H10-C]	[C20H10-B]/[C20H10-C]	[C20H10-D]/[C20H10-C]	[C20H10-E]/[C20H10-C]	[C20H10-F]/[C20H10-C]	
500	227	4.653E − 02	2.662E − 02	4.959E − 01	2.682E − 07	7.434E − 08	
700	427	7.045E − 02	8.194E − 02	6.229E − 01	3.839E − 05	1.213E − 05	
800	527	7.979E − 02	1.166E − 01	6.703E − 01	1.817E − 04	5.984E − 05	
900	627	8.768E − 02	1.536E − 01	7.103E − 01	6.091E − 04	2.074E − 04	
1000	727	9.439E − 02	1.915E − 01	7.444E − 01	1.605E − 03	5.611E − 04	
1100	827	1.001E − 01	2.295E − 01	7.739E − 01	3.546E − 03	1.268E − 03	
1200	927	1.051E − 01	2.669E − 01	7.996E − 01	6.870E − 03	2.502E − 03	
1300	1027	1.094E − 01	3.033E − 01	8.221E − 01	1.202E − 02	4.448E − 03	
1500	1227	1.165E − 01	3.723E − 01	8.599E − 01	2.945E − 02	1.118E − 02	

T (K)	T (°C)	[C20H12-A]/[C20H12-B]	[C20H12-C]/[C20H12-B]	[C20H12-D]/[C20H12-B]	[C20H12-E]/[C20H12-B]	[C20H12-F]/[C20H12-B]	[C20H12-G]/[C20H12-B]
500	227	1.247E − 01	4.403E − 03	2.287E − 06	3.700E − 07	2.076E − 08	3.458E − 05
700	427	2.363E − 01	1.965E − 02	9.873E − 05	3.712E − 05	4.666E − 06	8.513E − 04
800	527	2.887E − 01	3.139E − 02	3.231E − 04	1.580E − 04	2.557E − 05	2.335E − 03
900	627	3.376E − 01	4.520E − 02	8.155E − 04	4.893E − 04	9.639E − 05	5.136E − 03
1000	727	3.827E − 01	6.053E − 02	1.716E − 03	1.212E − 03	2.794E − 04	9.675E − 03
1100	827	4.242E − 01	7.687E − 02	3.159E − 03	2.549E − 03	6.688E − 04	1.627E − 02
1200	927	4.623E − 01	9.383E − 02	5.263E − 03	4.743E − 03	1.386E − 03	2.513E − 02
1300	1027	4.972E − 01	1.111E − 01	8.116E − 03	8.031E − 03	2.571E − 03	3.635E − 02
1500	1227	5.590E − 01	1.455E − 01	1.627E − 02	1.869E − 02	6.923E − 03	6.572E − 02

Table 4
Mole fraction of an equilibrium mixture of the PAH in Fig. 1 of a given empirical formula that is composed of the most stable PAH isomer (see text for discussion)

T (K)	T (°C)	Most stable PAH isomer for each empirical formula					
		C14H10-B	C16H10-A	C18H10-A	C18H12-D	C20H10-C	C20H12-B
500	227	0.9985	1.0000	0.9976	0.7724	0.6373	0.8856
700	427	0.9925	0.9999	0.9857	0.6961	0.5633	0.7956
800	527	0.9876	0.9996	0.9751	0.6637	0.5356	0.7559
900	627	0.9817	0.9989	0.9619	0.6342	0.5122	0.7198
1000	727	0.9751	0.9973	0.9467	0.6074	0.4920	0.6868
1100	827	0.9679	0.9943	0.9299	0.5829	0.4742	0.6563
1200	927	0.9605	0.9893	0.9120	0.5608	0.4582	0.6279
1300	1027	0.9529	0.9816	0.8932	0.5407	0.4435	0.6012
1500	1227	0.9378	0.9555	0.8538	0.5059	0.4166	0.5518

procedures are presented in Table 5. The ratio mol H_2/mol C_2H_2 is much higher than that found in combustion environments [5], so there could be less chemical driving force for MW growth in thermal treatment of soils. However, residence times for PAH–C_2H_2–H_2 contacting during soil thermal treatment are potentially considerably longer than those typical in flames ($\sim$ 10 ms). From a kinetic perspective this factor plus the possible catalytic activity of the soil could still create a chemical environment favorable to PAH MW growth reactions.

The ratio mol H_2/mol C_2H_2, or equivalently $p(H_2)/p(C_2H_2)$, is a key parameter in considering PAH growth [16]. However, there needs to be a way to determine either $p(H_2)$ or $p(C_2H_2)$. Bucalá et al. [19] measured C_2H_2, C_2H_4, and C_2H_6 yields. Using the same assumptions and calculation procedures as above, these total amounts can be converted into ratios of partial pressures of these three C_2 species.

The possibility that the C_2 hydrocarbons are in partial equilibrium was explored by considering the overall reaction:

$$2C_2H_4 = C_2H_2 + C_2H_6 \qquad (A)$$

The total amounts of C_2H_2, C_2H_4, and C_2H_6 were calculated from the kinetic parameters of Bucalá et al. [19], for a case corresponding to zero holding time in their experiments, i.e., cumulative yields generated by heating soil from room temperature to

Table 5
Relative amounts of C_2H_2 and H_2 evolved by pyrolysis of a Superfund-related soil matrix[a]

Table in Bucalá et al. [19]	Peak T (K)	Holding time(s)	wt.% C_2H_2	wt.% H_2	mol C_2H_2 / 100 g neat soil	mol H_2 / 100 g neat soil	mol H_2 / mol C_2H_2
3	1033	5	0.0162	0.095	6.22×10^{-7}	4.73×10^{-5}	76.1
4	1033	5	0.0096	0.157	3.68×10^{-7}	7.80×10^{-5}	211.6
5	955	0	0.0035	0.258	1.34×10^{-7}	1.28×10^{-4}	950.7

[a] Based on experimental data of Bucalá et al. [19] (see text for discussion).

a final (peak) temperature T_m, and then immediately beginning cool-down. Fig. 2 plots logarithmically against peak temperature, the quantity $[K_p(\text{exp})/K_p]$, where $K_p(\text{exp})$ is $[p_{C_2H_2}\, p_{C_2H_6}/(p_{C_2H_4})^2]$ a ratio of partial pressures calculated from Bucalá et al.'s experiments [19], and K_p is the same ratio of partial pressures calculated from free energies of formation using the thermochemical data of Table 2. Thermochemical properties for C_2H_2, C_2H_4, C_2H_6, and H_2 are taken from Kee et al. [25]. The partial pressures of the C_2 hydrocarbons deduced from experiment increasingly approach partial equilibrium, i.e., $\{K_p(\text{exp})/K_p = 1\}$, with increasing T_m. This suggests that at higher temperatures, reaction (A) cannot be ruled out as a source of acetylene in soil thermal treatment, assuming there is a plausible source of ethylene such as from decomposition of organic contaminant(s) or from pyrolysis of the soil itself [19]. Fig. 2 shows that the ratio $[K_p(\text{exp})/K_p] > 1$ for peak temperatures from 300°C to 1100°C. This implies that the experimental values of $p_{C_2H_2}$, $p_{C_2H_6}$ and $p_{C_2H_4}$ are not thermody-

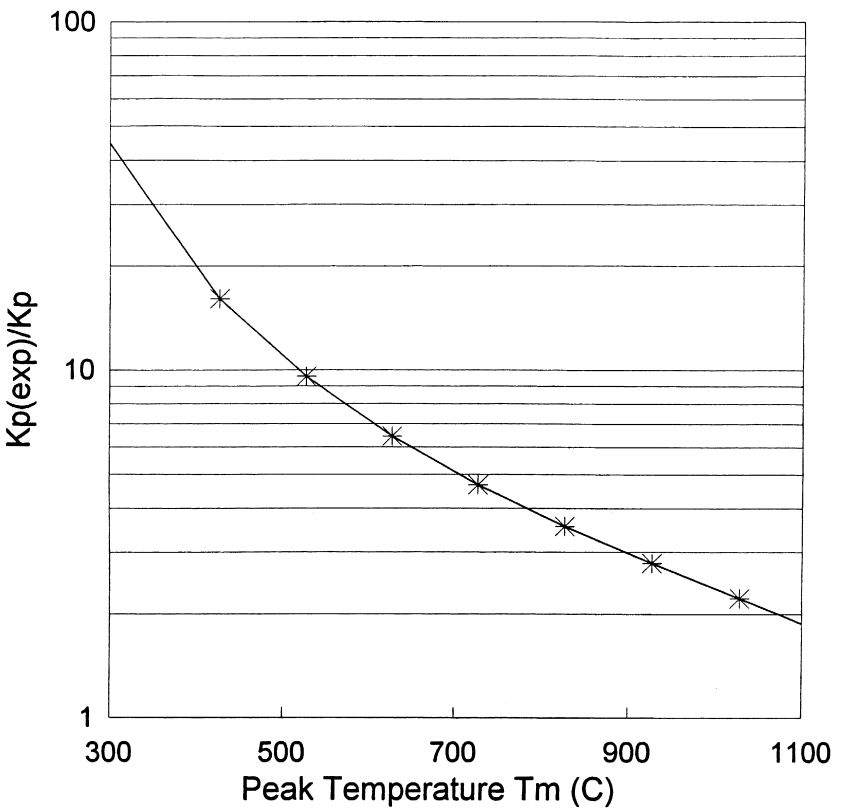

Fig. 2. Ratio of the experimental equilibrium constant, $K_p(\text{exp})$, to the thermodynamic equilibrium constant K_p, for the reaction $2C_2H_4 = C_2H_2 + C_2H_6$, as affected by peak temperature, T_m. The quantity $K_p(\text{exp}) = p_{C2H2}\, p_{C2H6}/(p_{C2H4})^2$ was calculated using partial pressures estimated from Bucalá et al.'s [19] experimental studies of the pyrolysis of uncontaminated soil; K_p was calculated from free energies of formation, using the thermochemical data of Table 2 (see text for discussion).

namically equilibrated, i.e., that $p_{C_2H_2}$ and/or $p_{C_2H_6}$ exceed, or $p_{C_2H_4}$ falls below, equilibrium value(s). The closer approach of K_p(exp) to K_p with increasing temperature (Fig. 2) is expected because slower kinetics at the lower temperatures inhibit thermodynamic equilibration.

Another method for estimating values for $p(H_2)$ needed for the PAH reaction calculations, is to use the derived relative partial pressures of C_2H_2, C_2H_4, and C_2H_6 to compute the $p(H_2)$ required for the following reactions to be in equilibrium:

$$C_2H_6 = C_2H_4 + H_2 \quad (a)$$

$$C_2H_4 = C_2H_2 + H_2 \quad (b)$$

$$C_2H_6 = C_2H_2 + 2H_2 \quad (c)$$

The resulting calculated values for $p(H_2)$ are shown in Fig. 3. There is considerable spread in the $p(H_2)$ values. At a given temperature, the $p(H_2)$ calculated from reaction (c) is the geometric mean of the $p(H_2)$ values calculated from reactions (a) and (b).

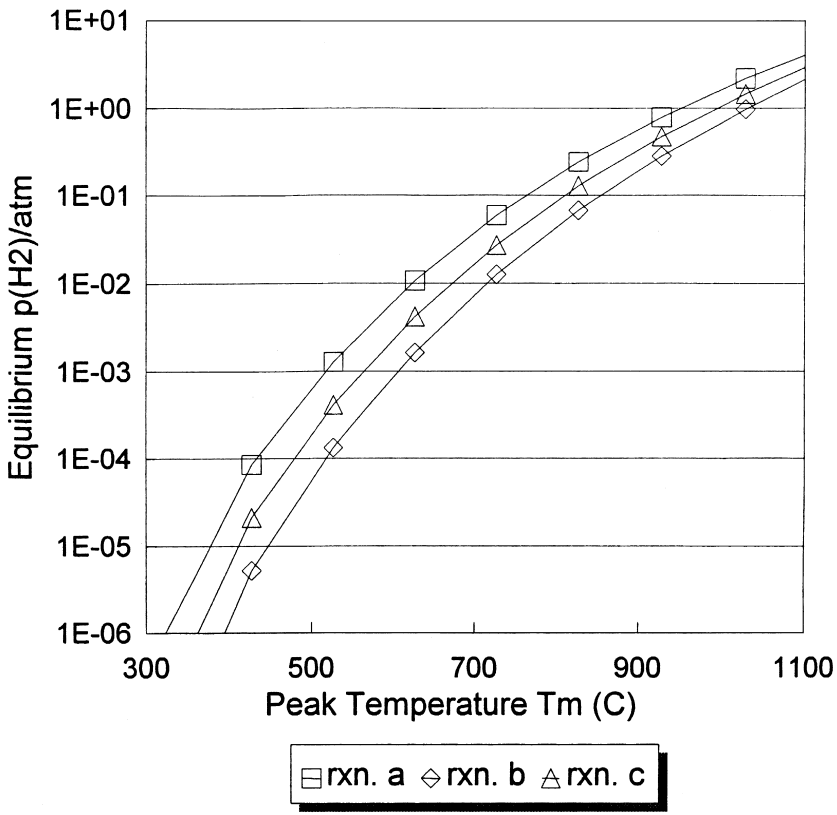

Fig. 3. Partial pressures of H_2, $p(H_2)$ in atm, calculated by assuming partial equilibrium for the reactions (a) $C_2H_6 = C_2H_4 + H_2$; (b) $C_2H_4 = C_2H_2 + H_2$; (c) $C_2H_6 = C_2H_2 + 2H_2$, using data from Bucalá et al. [19] to estimate the partial pressures of C_2H_2, C_2H_4, and C_2H_6 (see text for discussion).

Further, at a fixed temperature, the ratio of the $p(H_2)$ value calculated from reaction (a) to that from reaction (b) is equal to the ratio $K_p(\text{exp})/K_p$ plotted in Fig. 2. Therefore, the accuracy of using an equilibrium approximation to estimate $p(H_2)$ is limited by the extent to which the C_2 hydrocarbon concentrations themselves deviate from equilibrium. In the calculations below, the geometric mean value of $p(H_2)$ derived from equation (c), will be used. The equilibrium $p(H_2)$ exceeds 1 atm at higher values of T_m, which is physically unrealistic for the experimental conditions of Bucalá et al. [19]. Therefore, these equilibrium $p(H_2)$ values must be viewed as upper bounds for $p(H_2)$, at least at higher temperatures.

5. Overall reactions for PAH growth

Six overall reactions for PAH MW growth are listed in Table 6. Calling the PAH reactant P1 and the PAH product P2, the equilibrium constant, in terms of partial pressures $p(i)$ of reactant or product i, is, for reactions 1, 2, 3, and 6

$$K_p = \frac{p(\text{P2})\,p(H_2)}{p(\text{P1})\,p(C_2H_2)}$$

and, for reactions 4 and 5

$$K_p = \frac{p(\text{P2})\,p(H_2)}{p(\text{P1})\left[p(C_2H_2)\right]^2}$$

The thermodynamic driving force for growth can be seen in the ratio $K_p^* = p(\text{P2})/p(\text{P1})$. Setting $X = p(H_2)/p(C_2H_2)$,

$$K_p^* = \frac{K_p}{X}$$

for reactions 1, 2, 3, and 6, or

$$K_p^* = \frac{K_p}{X^2}\,p(H_2)$$

for reactions 4 and 5.

Table 6
Six representative PAH growth reactions

#	Reaction
1	C14H10-B + C_2H_2 = C16H10-A + H_2
2	C16H10-A + C_2H_2 = C18H10-A + H_2
3	C18H10-A + C_2H_2 = C20H10-C + H_2
4	C14H10-B + 2C_2H_2 = C18H12-E + H_2
5	C16H10-A + 2C_2H_2 = C20H12-B + H_2
6	C18H12-E + C_2H_2 = C20H12-B + H_2

Individual compounds are identified in Table 1.

To obtain an approximate lower bound for K_p^*, X is set to 1000 (roughly the largest value in Table 5 — see column 8). Using the values for $p(H_2)$ from reaction (c) in Fig. 3, the K_p^* for PAH growth reactions 1–6 as affected by temperature are plotted in Fig. 4. Even with this conservative assumption, the calculations predict that measurable amounts of product should form at all temperatures. The lowest predicted conversions, c. 1–5%, are for reactions 3 and 2, at the highest temperature, i.e., 1100°C. As would be expected, the predicted extents of PAH growth depend upon temperature. Because reaction rates increase with increasing temperature, kinetic limitations on the approach of reactions 1–6 to thermodynamic equilibrium are less at elevated temperatures. Thus, the predictions of Fig. 4 are expected to be in better accord with observation as temperature increases. Interestingly, the driving force for MW growth decreases with increasing temperature for all six reactions. The predicted extent of MW growth at all temperatures exhibits a strong dependence on the reaction pathway (Fig. 4). However, the six reactions divide into three separate pairs showing similar conversions at most temperatures from 400°C to 1100°C. These pairs are: reactions 1 and 6: net C_2 addition to a bay region forming a six-membered ring; reactions 2 and 3: net C_2 addition forming an ace ring; and reactions 4 and 5: a net addition of C_4H_2 forming a six-membered ring. These findings suggest that the MM3(92) thermochemical properties for these PAH might obey a group additivity relation.

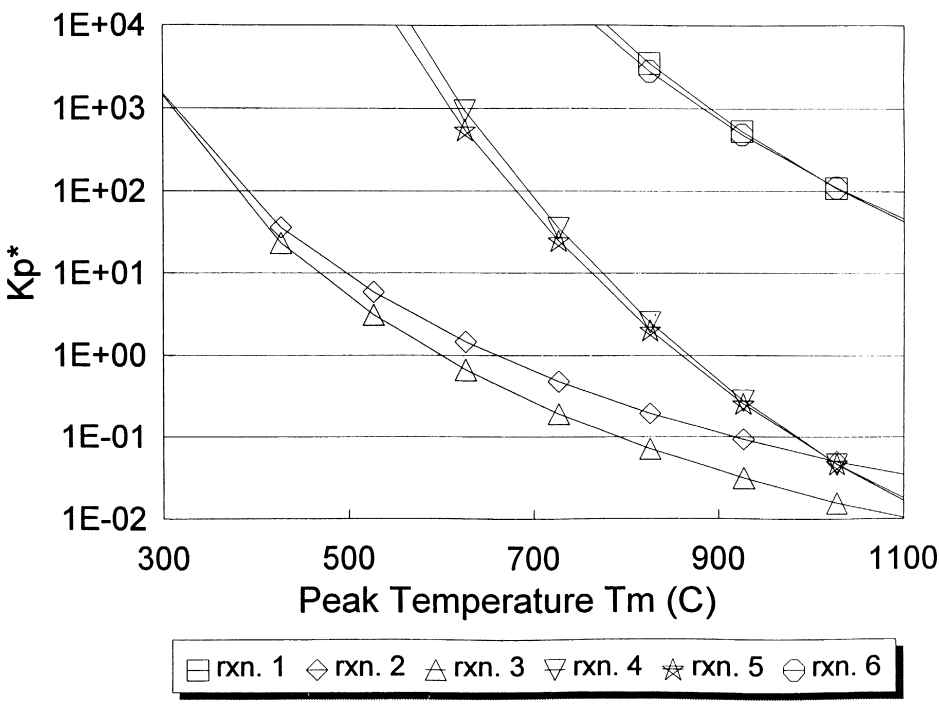

Fig. 4. Values of a thermodynamic driving force parameter, K_p^*, for PAH growth reactions 1–6 (Table 6) vs. T_m (see text for discussion).

6. Discussion

Environmentally significant chemical reactions of PAH, i.e., isomerizations and MW growth, are shown to be thermodynamically favored for temperatures and chemical environments pertinent to thermal treatment of polluted soils (Table 6, Fig. 4). For example, at equilibrium, several isomers of a PAH compound of a given empirical formula, not just the most stable species, can exist in significant inventories (Tables 3 and 4). Conservative calculations, i.e., that assume an appreciable inhibitory back-pressure of H_2 and an elevated temperature (1100°C) to reduce kinetic limitations, predict that unimolecular addition of acetylene to cyclopenta[*c*,*d*]pyrene (CPEP) and pyrene, respectively, convert about 1% and 8% of the parent PAH. Under the same conditions, predicted conversions from bimolecular addition of acetylene to phenanthrene or pyrene are about 2% to 4%, while unimolecular addition of acetylene to phenanthrene or triphenylene results in about 95% conversion of the substrate.

As discussed below, these and other results have implications for thermal cleaning of soils and other solids befouled by PAH. However, these implications must be understood in the context of the chemical environment investigated, i.e., PAH thermal reactions in the absence of oxygen. Our calculations are not designed to forecast the performance of large-scale thermal treatment processes in removing PAH from soil, or in limiting adverse effluents. It is common for such technologies to subject soil-derived volatiles to high temperature oxidation and/or other cleaning measures, e.g., downstream after-burners, adsorption on activated carbon. Further, in practical-scale equipment, transport resistances typically confound the effects of purely chemical phenomena. Nevertheless, the present findings are relevant to understanding certain attributes of current and future thermally based methods for cleaning PAH-polluted soils. Studies of oxygen-free conditions provide a reference case for differentiating O_2-induced effects. They also help diagnose and interpret off-spec performance of oxidative systems when desired oxygen potentials are vitiated, e.g., because of mixing imperfections, temperature excursions, under-feeding of oxidant, and overfeeding of soil. They also shed light on the behavior of non-oxidative thermal technologies, e.g., treatment in thermal plasmas, baths of molten material, etc.

PAH compounds relevant to those encountered at Superfund and other contaminated waste sites, i.e., compounds of empirical formulas $C_{14}H_{10}$ to $C_{20}H_{12}$ (Table 1, Fig. 1) were studied. Among these was pyrene, $C_{16}H_{10}$. Pyrene has been found in complex organic mixtures at hazardous waste sites, e.g., heavy oils, sludges, or tars [17]. Pyrene and the other compounds in Table 1 and Fig. 1 have a MW, volatility, and thermal chemical reactivity pertinent to mid-boiling range PAH, an important class of soil contaminants at least some of which can be resistant to biochemical degradation.

Other connections exist to practical soil cleaning methods. The temperature range studied (400–1100°C) is encountered in various practical processes. Further, the role of acetylene in PAH MW growth received close attention, reflecting the presence of acetylene during thermal decontamination of at least some soils. For example, C_2H_2 has been identified [19] as a product of the thermal decomposition of uncontaminated specimens of a synthetic soil matrix prepared for the US EPA to reflect attributes of soils at US Superfund sites [20]. Further, it is well known that C_2H_2, among other

products, is generated by thermal decomposition of aromatics above about 1000 K [26]. Acetylene and other light hydrocarbons are reported as products from anthracene pyrolysis at ≥ 1200 K [27]. For a given temperature and chemical environment, the present predictions constitute a limiting case because they assume thermodynamic equilibrium, i.e., that chemical kinetic and transport resistances are all negligible. In practical systems, it is almost inevitable that limitations on rates of chemical reactions, species mixing and mass transfer, or heat transmission, will impact some aspect of process performance. Nevertheless, an understanding of equilibrium conditions provides a valuable benchmark for comparing observations and discerning the severity of kinetic limitations on the attainment of equilibrium. Rates of PAH thermal reactions increase with increasing temperature, so in general, equilibrium predictions are expected to be more reliable at higher temperatures. We are unaware of side-by-side comparisons between equilibrium predictions and experimental determinations of PAH thermal reaction behavior. However, there are supporting experimental data. Mukherjee et al. [28] and Mulholland et al. [29] identified PAH products from pyrolysis of aromatic hydrocarbons of interest as model compounds for fuels and wastes, e.g., pyrene from 1200 to 1500 K [28], *o*-dichlorobenzene, toluene, or mixtures thereof from 1100 to 1500 K [29]. They propose isomerization, or acetylene addition, or both pathways as important channels for PAH pyrolysis at elevated temperatures (see further discussion below).

During soil thermal treatment an individual PAH contaminant is predicted to be transformed to other PAH isomers (Tables 3 and 4), and to new PAH by MW growth owing to acetylene addition (Table 6, Fig. 4). Several of these MW growth reactions are of particular environmental health interest because they involve conversion of non-mutagens to mutagens and vice versa. By a "mutagen" we mean a substance, here an individual PAH compound, that scores positively in a bacterial cell [1] or a human cell [2] in vitro forward mutation assay. It is recognized that some environmental health scholars are not convinced of an unequivocal link between every case of mutagenicity in single cell model systems, and genetic or other morbidity in humans. Nevertheless, it is prudent to draw attention to chemical changes that modify the inventory of PAH that exhibit in vitro bioactivity. In this regard four reactions in Table 6 and Fig. 4 command particular attention. Reaction (2) shows the non-mutagen pyrene being transformed to CPEP which exhibits bacterial cell and human cell mutagenicity. In reaction (3) CPEP is converted to dicyclopenta[*cd*, *fg*]pyrene, a PAH that to our knowledge has not been tested for mutagenicity in either of the above model systems. Fig. 4 shows that both of these reactions become increasingly less thermodynamically favored with increasing temperature, but that reaction (2) retains appreciably more driving force than reaction (3). The latter implies that competition between reactions (2) and (3) favors CPEP accumulation. These calculations are in accord with experimental observations from other studies. Mulholland et al. [29] identified phenanthrene, pyrene, and CPEP among the products of *o*-dichlorobenzene pyrolysis at 1460 K, and proposed that pyrene and CPEP were, respectively, formed by acetylene addition to phenanthrene [see reaction (1), Table 6] and to pyrene [see reaction (2), Table 6]. Richter et al. [30] found CPEP as a product of heating pure pyrene under helium at 1000°C. Interestingly for similar conditions, CPEP yields were over 15-fold higher from heating a mixture of pyrene with

sand or of pyrene with a Superfund-related soil matrix, but no PAH were detected from heating uncontaminated soil [30]. Catalysis of pyrene conversion to CPEP by silica minerals in the soil is a plausible explanation. Reaction (4), by addition of two acetylene molecules, transforms the non-mutagen phenanthrene to triphenylene, a human cell mutagen. However, reaction (6) converts triphenylene to benzo[*e*]pyrene, for which we do not have in vitro mutagenicity test information (Table 1). Fig. 4 implies substantially greater thermodynamic driving potential for reaction (6) vs. reaction (4) at all temperatures, so that according to equilibrium, little net build-up of triphenylene would be expected.

At equilibrium, isomerization may substantially complicate the contamination caused by an individual PAH compound. Table 4 shows that the mole fraction of an equilibrium mixture of PAH of the same empirical formula accounted for by the most thermodynamically stable isomer declines with increasing temperature. Table 3 presents, for each of the stable isomers of Table 4, the equilibrium molar ratio of other isomers to that stable isomer, for a range of temperatures. The fractional contributions of all other isomers increase with increasing temperature. Table 3 shows two cases where at equilibrium, mutagenic PAH isomers would coexist with a more stable non-mutagenic PAH: (1) for the $C_{16}H_{10}$ system, the bacterial mutagens fluoranthene (-B, Table 1) and acephenanthrylene, cyclopenta[*j*,*k*]phenanthrene (-C) coexist with pyrene (-A); (2) for the $C_{20}H_{12}$ system, benzo[*b*]fluoranthene (-G) a human cell mutagen, and benzo[*a*]pyrene (BaP) (-A, Table 1) the well known bacterial cell and human cell mutagen, coexist with benzo[*e*]pyrene (-B). BaP is of particular environmental health interest because it is biochemically linked to human lung carcinoma [31]. Note that the calculations predict increasing relative abundance for these bioactive PAH in their respective isomeric mixtures as temperature increases. Table 3 also shows that at equilibrium, one or more additional mutagens would coexist with a most stable and mutagenic isomer: (1) for the $C_{18}H_{10}$ system the bacterial cell mutagen benzo[*ghi*]fluroanthene (-B, Table 1) would coexist with CPEP (-A); (2) for the $C_{18}H_{12}$ system three different human cell mutagens benzo[*a*]anthracene (-B, Table 1), benzo[*c*]phenanthrene (-C), and triphenylene (-E) would coexist with chrysene (-D). If MW growth by acetylene addition is followed by isomerization, a non-mutagenic PAH may be transformed to one or more mutagens. For example, acetylene addition to phenanthrene, a non-mutagen, to produce pyrene, another non-mutagen [reaction (1), Table 6], has a strong thermodynamic driving force at all temperatures (Fig. 4). However, as noted above, pyrene isomerization to two different bacterial cell mutagens becomes increasingly favored at equilibrium, at higher temperatures (Table 3), suggesting a two-step process to transform phenanthrene to mutagens if acetylene is available. Similarly, the possible reduction in PAH mutagenicity attainable by converting triphenylene to benzo[*e*]pyrene by acetylene addition [reaction (6), Table 6], may be offset by isomerization of the BeP to the toxicants BaP and benzo[*b*]fluoranthene, as discussed above.

Experimental observations are consistent with the present predictions of an important role for isomerization. Mukherjee et al. [28] found CPEP and cyclopenta[*hi*]acephenanthrylene (CPAP) [$C_{18}H_{10}$-F, Table 1] as products of pyrene pyrolysis from about 1300 to 1500 K, with CPEP increasing monotonically over this temperature range but CPAP maximizing at about 1400 K. They proposed [28] CPAP

isomerization as an important pathway for CPEP production at higher reaction severities. This would be consistent with the equilibrium predictions of Table 3, column 7, showing modest equilibrium ratios of CPAP to CPEP, even at Mukherjee et al.'s [28] highest temperature of about 1500 K. In explaining PAH product spectra from *o*-dichlorobenzene pyrolysis at 1460 K, Mulholland et al. [29] hypothesized benzo[*ghi*]fluoranthene [$C_{18}H_{10}$-B, Table 1], as one of their unknown products, and further proposed that this PAH formed by isomerization of CPEP. Table 3, column 3, shows that significant thermodynamic driving force for CPEP isomerization to $C_{18}H_{10}$-B is predicted for the 1200 to 1500 K temperature range. Mulholland et al. [29] also proposed that another unknown 1460 K product was dicylcopenta[*cd, jk*]pyrene [$C_{20}H_{10}$-D, Table 1], formed by acetylene addition to CPEP. They did not report dicylcopenta[*cd, fg*]pyrene [$C_{20}H_{10}$-C, Table 1], the most thermodynamically stable PAH of this $C_{20}H_{10}$ set (Table 3) as a product. Above 600°C, Fig. 4 shows only modest thermodynamic driving force for production of $C_{20}H_{10}$-C by acetylene addition to CPEP [reaction (3), Table 6]. However, Table 4 shows that $C_{20}H_{10}$-C loses considerable thermodynamic stability with increasing temperature and Table 3, column 5, shows that with increasing temperature $C_{20}H_{10}$-D becomes an increasingly important isomer in this set, exhibiting equilibrium concentrations that approach those of isomer-C (i.e., $> 83\%$ of -C) at Mulholland et al.'s temperature of 1460 K.

7. Conclusions

Despite the structural complexity of PAH and, for higher MW species, their significant number of isomers, molecular mechanics methods [MM3(92)] can be used to estimate thermochemical properties that allow calculation of equilibrium constants for PAH chemical reactions as a function of temperature. This information in turn can be employed to predict, for the limiting case of thermodynamic equilibrium, the importance of thermal chemical reactions that modify PAH structure and bioactivity. This paper examined two classes of such reactions, MW growth by acetylene addition and intramolecular rearrangement (isomerization). PAH with empirical formulae $C_{14}H_{10}$, $C_{16}H_{10}$, $C_{18}H_{10}$, $C_{18}H_{12}$, $C_{20}H_{10}$, and $C_{20}H_{12}$ were studied. For all six PAH empirical formulae the calculations predict that with increasing temperature isomerization increases the "complexity" of the PAH mixture, i.e., as temperature rises the relative abundance of all PAH isomers in the mixture other than the most stable isomer increases. Isomerization also partially transforms non-mutagens to mutagens, e.g., pyrene and benzo[*e*]pyrene to fluoranthene and benzo[a]pyrene (BaP), respectively, and partially converts cyclopenta[c,d]pyrene (CPEP) and chrysene, both human cell mutagens, to one and three additional human cell mutagens, respectively. Acetylene addition transforms the non-mutagens phenanthrene and pyrene to the mutagens triphenylene and CPEP, respectively. Acetylene addition also transforms mutagens to non-mutagens, e.g., triphenylene to benzo[*e*]pyrene (BeP) but BeP isomerization may then give rise to bioactive compounds including BaP.

These results are of interest to research, and to practical scale studies of thermal decontamination of hazardous substances including soils. PAH are common exogenous

contaminants of soils, and acetylene has been observed as a product of heating soil. The present predictions assume thermodynamic equilibrium in an oxygen-free system. They do not shed light on kinetics or on oxidative reactions. They do provide a limiting case for comparison with experimental and kinetic modeling results under similar conditions of temperature and chemical environment. Such conditions may arise in commercial practice owing to accidental or intentional vitiation of oxygen. This work demonstrates that during thermal treatment in the absence of oxygen there is no inherent chemical prohibition to the transformation of stable, non-mutagenic PAH to mutagens and even carcinogens in the case of BeP to BaP. Some of the predicted PAH have been observed elsewhere among the products of aromatics pyrolysis at elevated temperatures [28–30]. In summary, our predictions elucidate PAH thermal reactivity for comparisons with measurements and kinetics modeling calculations, and for practical waste treatment processes, identify PAH chemistries to be monitored and where necessary counteracted by engineering design and auxiliary cleaning methods. The identification and testing of such technological countermeasures are not the objectives of the present paper. However, in light of prior knowledge and results of the present study, examples of plausible methodologies are: appending or interdicting soil pyrolysis by oxidation, e.g., in the main heating chamber and/or in immediately downstream afterburners; and adsorption of PAH that escape the thermal treatment chamber(s) on active carbon (for subsequent further cleaning). Also important are methods for real-time, on-line detection of PAH in the treatment chamber and its effluent streams, e.g., laser-induced fluorescence (LIF), see Refs. [32,33]. The efficaciousness of PAH countermeasures and monitoring technologies in soil thermal decontamination applications should be evaluated at scales appropriate to their intended use.

Acknowledgements

The authors thank Prof. Patrick Gilot, and Drs. Arthur Lafleur and Henning Richter for helpful discussions. Financial support of this research by the National Institute of Environmental Health Sciences Grant ES04675 (MIT-Superfund Hazardous Substances Basic Research Program) is gratefully acknowledged.

References

[1] J.B. Howard, J.P. Longwell, J.A. Marr, C.J. Pope, W.F. Busby Jr., A.L. Lafleur, K. Taghizadeh, Combust. Flame 101 (1995) 262–270.
[2] J.L. Durant, W.F. Busby Jr., A.L. Lafleur, B.W. Penman, C.L. Crespi, Mutat. Res. 371 (1996) 123–157.
[3] M. Frenklach, D.W. Clary, W.C. Gardiner, S.E. Stein, Proceedings, Twentieth Symposium (International) on Combustion, The Combustion Institute, Pittsburgh,1984, pp. 887–901.
[4] M. Frenklach, J. Warnatz, Combust. Sci. Technol. 51 (1987) 265–283.
[5] J.A. Marr, PhD, Thesis, Department of Chemical Engineering, Massachusetts Institute of Technology, Cambridge, MA, 1993.
[6] L.T. Scott, N.H. Roelofs, J. Am. Chem. Soc. 109 (1987) 5461.
[7] A.J. Stone, D.J. Wales, Chem. Phys. Lett. 128 (1986) 501.
[8] S. Macadam, PhD Thesis, Department of Chemical Engineering, Massachusetts Institute of Technology, Cambridge, MA, 1997.

[9] L. Brouwer, J. Troe, Int. J. Chem. Kinet. 20 (1988) 379.
[10] N.L. Allinger, F. Li, L. Yan, J.C. Tai, J. Comput. Chem 11 (1990) 868.
[11] H.-D. Beckhaus, S. Verevkin, C. Rüchardt, F. Diedrich, C. Thilgen, H.-U. ter Meer, H. Mohn, W. Müller, Angew. Chem., Int. Ed. Engl. 33 (1994) 996.
[12] C.J. Pope, J.B. Howard, J. Phys. Chem. 99 (1995) 4306.
[13] Y. Jin, J. Cheng, M. Varma-Nair, G. Liang, Y. Fu, B. Wunderlich, X.-D. Xiang, R. Mostovoy, A.K. Zettl, J. Phys. Chem. 96 (1992) 5151.
[14] C.J. Pope, J.B. Howard, Department of Chemical Engineering, Massachusetts Institute of Technology, Cambridge, MA, unpublished results.
[15] D.M. Ho, R.A. Pascal Jr., Chem. Mater. 5 (1993) 1358–1361.
[16] C.J. Pope, J.B. Howard, Tetrahedron 52 (1996) 5161–5178.
[17] H.H. Saito, PhD, Thesis, Department of Chemical Engineering, Massachusetts Institute of Technology, Cambridge, MA, 1995.
[18] H.H. Saito, V. Bucalá, J.B. Howard, W.A. Peters, Environ. Health Perspect. 106 (Suppl. 4) (1998) 1097–1107.
[19] V. Bucalá, H. Saito, J.B. Howard, W.A. Peters, Ind. Eng. Chem. Res. 35 (1996) 2725–2734.
[20] R.M. Frederick, US EPA, Personal communication, 1993.
[21] US EPA, "Development and Use of EPA's Synthetic Soil Matrix (SSM/SARM)", US EPA, Releases Control Branch, Risk Reduction Engineering Laboratory, Edison, NJ, 1989.
[22] P. Esposito, J. Hessling, B.B. Locke, M. Taylor, M. Szabo, R. Thurnau, C. Rogers, R. Traver, E. Barth, J. Air Pollut. Control Assoc. 39 (3) (1989) 294–304.
[23] J.B. Pedley, R.D. Naylor, S.P. Kirby, Thermochemical Data of Organic Compounds, 2nd edn., Chapman & Hall, London, 1986.
[24] E. Ritter, J.W. Bozzelli, Int. J. Chem. Kinet. 23 (1991) 767–778.
[25] R.J. Kee, F.M. Rupley, J.A. Miller, The Chemkin Thermodynamic Data Base, Report No. SAND87-8215B, Sandia National Laboratory, Livermore, CA, 1990.
[26] G. Egloff, Reactions of pure hydrocarbons, ACS Monogr. (1937) American Chemical Society, Washington, DC.
[27] M.J. Wornat, A.F. Sarofim, A.L. Lafleur, Proceedings, Twenty-Fourth Symposium (International) on Combustion, The Combustion Institute, Pittsburgh, 1992, pp. 955–963.
[28] J. Mukherjee, A.F. Sarofim, J.P. Longwell, Combust. Flame 96 (1994) 191–200.
[29] J.A. Mulholland, A.F. Sarofim, J.M. Beér, A.L. Lafleur, Proceedings, Twenty-Fourth Symposium (International) on Combustion, The Combustion Institute, Pittsburgh, 1992, pp. 1091–1099.
[30] H. Richter, V. Risoul, A.L. Lafleur, E.F. Plummer, J.B. Howard, W.A. Peters, Chemical characterization and bioactivity of polycyclic aromatic hydrocarbons (PAH) from non-oxidative thermal treatment of pyrene-contaminated soil at 250–1000°C, Environ. Health Perspect. (2000) in press.
[31] M.F. Denissenko, A. Pao, M.S. Tang, G.P. Pfeifer, Science 247 (1996) 430.
[32] J.H. Thijssen, M.A. Toqan, J.M. Beér, A.F. Sarofim, Combust. Sci. Technol. 90 (1993) 101–110.
[33] J.H. Thijssen, M.A. Toqan, J.M. Beér, A.F. Sarofim, Proceedings, Twenty-Fifth Symposium (International) on Combustion, The Combustion Institute, Pittsburgh, 1994, pp. 1215–1222.